

Research paper

Edge-based SEIR dynamics with or without infectious force in latent period on random networks



Yi Wang^{a,b,c,*}, Jinde Cao^{c,d}, Ahmed Alsaedi^e, Bashir Ahmad^e

^a School of Mathematics and Physics, China University of Geosciences, Wuhan 430074, China

^b Department of Mathematics and Statistics, University of Victoria, Victoria BC V8W 3R4, Canada

^c Department of Mathematics, Southeast University, Nanjing 210096, China

^d Department of Mathematics, Faculty of Science, King Abdulaziz University, Jeddah 21589, Saudi Arabia

^e Nonlinear Analysis and Applied Mathematics (NAAM) Research Group, Department of Mathematics, Faculty of Science, King Abdulaziz University, Jeddah 21589, Saudi Arabia

ARTICLE INFO

Article history:

Received 7 May 2015

Revised 29 August 2016

Accepted 20 September 2016

Available online 28 September 2016

Keywords:

SEIR models

Latent period

Final epidemic size

Random networks

Probability generating function

Stochastic simulations

ABSTRACT

In nature, most of the diseases have latent periods, and most of the networks look as if they were spun randomly at the first glance. Hence, we consider SEIR dynamics with or without infectious force in latent period on random networks with arbitrary degree distributions. Both of these models are governed by intrinsically three dimensional nonlinear systems of ordinary differential equations, which are the same as classical SEIR models. The basic reproduction numbers and the final size formulae are explicitly derived. Predictions of the models agree well with the large-scale stochastic SEIR simulations on contact networks. In particular, for SEIR model without infectious force in latent period, although the length of latent period has no effect on the basic reproduction number and the final epidemic size, it affects the arrival time of the peak and the peak size; while for SEIR model with infectious force in latent period it also affects the basic reproduction number and the final epidemic size. These accurate model predictions, may provide guidance for the control of network infectious diseases with latent periods.

© 2016 Elsevier B.V. All rights reserved.

1. Introduction

The idea of mathematical methods to epidemiology was pioneered by Daniel Bernoulli [1], who focused on the effect of variolation against smallpox to prolong life expectancy. This topic, termed by mathematical epidemiology (ME), didn't have much achievement in the late eighteenth and nineteenth centuries until the early twentieth century. In 1911, Sir Ross developed a mathematical model to capture the spread of malaria, a disease which is transmitted via mosquitoes, and proposed a central concept "threshold effect" in epidemiology, highlighting that the malaria in a region could be eliminated through reducing the mosquito population [2]. This idea was further formalized and generalized to a large class of diseases by Kermack and McKendrick [3] in 1927, known as the basic reproduction number or basic reproductive ratio and usually denoted as R_0 in epidemiology, which quantifies the expected number of secondary cases generated by a typical infected individual during its entire infectious period while introduced to a fully susceptible population [4]. Since then, numerous

* Corresponding author.

E-mail addresses: wangyi-mail@163.com (Y. Wang), jdcg@seu.edu.cn (J. Cao), aalsaedi@hotmail.com (A. Alsaedi), bashirahmad_qau@yahoo.com (B. Ahmad).

mathematical models have been proposed to study the spread and control of infectious diseases, using R_0 as an important indicator, see [5] and [6], for example.

Two fundamental models commonly used in mathematical epidemiology are the so called susceptible-infected-recovered (SIR) and susceptible-infected-susceptible (SIS) models. For SIR models, susceptible individuals become infectious immediately once infected, and the infected individuals become fully immune once recovered (here, we use R to denote the recovered individuals; however, some authors also use R to denote the removal individuals that are either through the isolation or through death caused by the disease. In both cases, the recovered or removal individuals play no role in transmitting infection, and thus they are equivalent from a modeling point of view); while for SIS models, the infected individuals become fully susceptible that can be re-infected again. Usually, SIR models are appropriate for diseases such as influenza and measles caused by a virus, while SIS models are appropriate for diseases such as syphilis and gonorrhoea caused by a bacteria [7,8].

For the SIR model without demographic, if $R_0 < 1$, the infection decays directly and there is no epidemic prevalence; otherwise, the infection goes up at first as individuals get infected, then down again as they recover, and there is an outbreak. The whole process ends with no infection in the limit of large time t [7,8]. In addition, the final epidemic size, i.e. the total people affected by the disease in the end, is given by an implicit equation [3].

It should be mentioned that the classical SIR/SIS model implicitly assumes that the population is homogeneously mixed, i.e. every individual in the population has the same probability of contacting any other individual. This is obvious not the case in the real world. In fact, different individual may have varying number of contacts. This idea was initiated by Diekmann et al.[9]. Although Diekmann et al.[9] mainly considered the homogeneous population in which each individual had exactly the same number of k acquaintances, they pointed out in the concluding remarks that individuals might have different number of acquaintances, the situation pioneered by Pastor-Satorras and Vespignani [10] on epidemics in heterogeneous networks.

Indeed, contact network models are more realistic to describe the population mixing pattern. Under such framework, each individual of the population is denoted by a node, and possible contacts between two individuals are linked by an edge between the corresponding two nodes of the network; these two nodes are neighbors of each other. In [11], Moreno et al. considered the SIR model in complex heterogeneous networks, and obtained the following basic reproduction number

$$R_0 = \frac{\beta \langle k^2 \rangle}{\gamma \langle k \rangle}, \quad (1)$$

where β is the transmission rate along per edge, γ is the constant recovery rate of infected individuals, $\langle k \rangle = \sum_k k P(k)$ is the average degree of the network, and $\langle k^2 \rangle = \sum_k k^2 P(k)$ is the second moment of the degree distribution $P(k)$. Moreover, they obtained the final size equations on various networks.

Network SIR models have been further studied by several authors in the literature. For example, by using a combination of bond percolation and generating function methods, Newman [12] derived the epidemic threshold and the final epidemic size. The basic reproduction number in [12] is defined as

$$R_0 = \frac{\beta}{\beta + \gamma} \frac{\langle k(k-1) \rangle}{\langle k \rangle} = \frac{\beta}{\beta + \gamma} \left(\langle k \rangle - 1 + \frac{\text{Var}[k]}{\langle k \rangle} \right), \quad (2)$$

where $\text{Var}[k]$ denotes the variance of network degree distribution. The first factor of (2) describes the fact that an infected node spreads out the infection before it recovers, and the second factor is the average excess degree of the network. However, different from a dynamical model, one limitation of this mapping method is that it can not give us the dynamical evolution of a disease. Lindquist et al. [13] introduced effective degree SIR and SIS models on a contact network, and obtained the same basic reproduction number R_0 for network SIR model as (2).

Considering infection across the edge, Keeling [14] proposed an edge-based SIR model on homogeneous networks, which leads to a basic reproduction number different from (2) since it takes the multiplicative correlation between connected nodes of various types into account. This formalism is further extended to SIR model on heterogeneous networks by adopting all combinations of degree pairs as variables [15], but it is very difficult to analyze (in fact, the dimension for the differential equations is of quadratic order of maximum degree of the network). Recently, using the probability generating function (PGF) method, Volz [16] considered SIR epidemics on random networks, and derived a system of three nonlinear ordinary differential equations (ODEs), the predictions of which agrees excellent well with the stochastic SIR simulations. By slightly modifying the definition of parameters, Miller [17] further showed that an SIR model on random networks was intrinsically two dimensional, which is consistent with the classical homogeneously mixed model. Both the models of Volz [16] and Miller [17] yield the same basic reproduction number as (2). There are lots of extensions using this edge-based compartmental modeling approach, see, e.g., [18–22].

However, in reality, many diseases have latent or incubation periods, i.e. individuals first entering an exposed class E and having no apparent symptoms, the length of which varies from disease to disease. For example, measles has a 8–13-day latent period, influenza has only a 1–3-day latent period, and Acquired Immune Deficiency Syndrome (AIDS) has the incubation time ranging from a few months to years after the patient has been shown to get antibodies to the human immunodeficiency virus (HIV) [23]. One can incorporate this effect by adding a new class E to the classical SIR model. During the latent period, the susceptible once infected remains no symptom for a certain length of time before entering the infective class I, and the individuals may or may not have infectious force depending on the particular disease under

consideration. A number of authors have considered SEIR models in homogeneously mixed populations and studied their global dynamics in detail [24–28], to name a few.

In [29], considering an age of infection model such as SARS epidemic, Brauer got the following SEIR model

$$\begin{cases} S' = -\beta(N)S(I + \epsilon E), \\ E' = \beta(N)S(I + \epsilon E) - \nu E, \\ I' = \nu E - \gamma I, \\ R' = \gamma I, \end{cases} \quad (3)$$

where $\beta(N)$ is the general contact rate, $1/\nu$ is the length of latent period, and $0 \leq \epsilon < 1$ is a reduced factor if individuals have infectious force during the latent period. If $\epsilon = 0$, there is no infectivity during the latent period. As argued above for the classical SIR model, model (3) completely ignores the population structure. The first attempt is to consider SEIR models on random contact networks. Several authors conduct such modifications and extensions. Liu and Zhang [30] studied the threshold and permanence of an SEIRS epidemic in scale-free networks. Jin et al. [31] formulated a network SEAIR model to estimate the spread and control of pandemic influenza A (H1N1). Combining with the high-resolution data, Stehlé [32] et al. simulated an SEIR infectious disease model on a dynamic contact network among conference attendees. Zhu et al. [33] investigated the global stability of a generalized SEIR epidemic model on heterogeneous networks. Shang [34] formulated a SEIR model without infectious force in the latent period on random networks with arbitrary degree distribution. However, all of these network SEIR models are node-based, and are not compared with stochastic SEIR simulations. To our knowledge, only Shang [34] extended the edge-based SIR modeling approach in [17] to SEIR dynamics, the point of which was also mentioned in [19].

The SEIR dynamics without infectious force in the latent period on random networks is also considered in [34]. We extend the model of [34] in three respects. First, we correct a term of the network SEIR model in [34] to let the predictions of the model be more accurate when comparing with the stochastic simulations. Second, we also allow the infectious force with a reduced factor in the latent period; note that the infectious force in the latent period is not covered in [34]. Thirdly, we perform large-scale stochastic simulations, including different initial conditions of the infectives, lengths of latent period and types of networks, to compare with the predictions of our models.

The remaining part of the paper is structured as follows. Section 2 first gives a brief review of SIR dynamics on random networks, and then formulates SEIR models with or without infectious force in the latent period. These models are described by a small number of nonlinear system (intrinsically only three dimensional) of ordinary differential equations, completed with appropriate initial conditions; the basic reproduction numbers and the final epidemic size formulae are also given. In Section 3, large-scale simulations are performed to compare the predictions of ordinary differential equation systems with stochastic simulations on random networks. Section 4 concludes the paper with some remarks.

2. Epidemic dynamics

When modeling epidemic dynamics on complex networks, especially on heterogeneous networks, one should take the degree fluctuations into account. In the next subsection, we briefly give the modelling idea of SIR dynamics on random networks.

2.1. The basic SIR dynamics on random networks

In the course of an SIR epidemic spreading, what we are concerned is the fraction of the population that has not yet been infected. This is equivalent to the probability that an individual chosen uniformly at random from the population is still susceptible at time t . Consider a susceptible node of degree k at initial time t_0 . This node can receive infection only along one of its k edges if there is one or more infectious neighbors. For the ease of statement, we call this node *the target node u*. Let $\theta(t)$ and $\phi(t)$ be the probability, respectively, that a random edge has not admitted infection and an edge has not admitted infection and its base node is infectious at time t .

Thus, by assuming independence, the probability that the target node u of degree k doesn't become infected is θ^k . Then, we have the following SIR model on random networks [17,35]

$$\begin{cases} \theta' = -\beta\phi, \\ \phi' = -(\beta + \gamma)\phi - \frac{\Psi''(\theta)}{\Psi'(1)}\theta' = -(\beta + \gamma)\phi + \beta\phi\frac{\Psi''(\theta)}{\Psi'(1)}, \\ S(t) = \sum_{k=0}^{\infty} P(k)\theta(t)^k = \Psi(\theta(t)), \\ I' = -S' - \gamma I = \beta\phi\Psi'(\theta) - \gamma I. \end{cases} \quad (4)$$

where $\Psi(x) = \sum_{k=0}^{\infty} x^k P(k)$ is the probability generating function of degree distribution $P(k)$. Note that $\Psi(1) = \sum_k P(k) = 1$ and $\Psi'(1) = \sum_k kP(k) = \langle k \rangle$.

The basic reproduction number for model (18) is

$$R_0 = \frac{\beta}{\beta + \gamma} \frac{\Psi''(1)}{\Psi'(1)} \doteq T \frac{\Psi''(1)}{\Psi'(1)}, \quad (5)$$

where T denotes the probability that an infectious base node spreads the infection to a susceptible target node before it recovers, and $\Psi''(1)/\Psi'(1)$ is the average excess degree of a target node. The expression (5) for R_0 is the same as (2) obtained by the bond percolation method [12] and the effective degree approach [13].

The final epidemic size is given by

$$\theta_\infty = \frac{\beta \frac{\Psi'(\theta_\infty)}{\Psi'(1)} - \beta \phi_0 + \gamma}{\beta + \gamma},$$

where $\theta_\infty = \theta(\infty)$ is the probability that a randomly chosen node u escapes from the infection at the end of the epidemic. Then, $S(\infty) = \sum_{k=0}^{\infty} P(k)\theta_\infty^k = \Psi(\theta_\infty)$. Hence, the final size of an epidemic is $R(\infty) = 1 - S(\infty)$.

2.2. SEIR Dynamics without infectious force in the latent period

In this subsection, we consider the SEIR dynamics without infectious force in the latent period. Unlike the above SIR model where susceptible individuals become infectious instantly once infected, susceptible individuals enter an infected phase but have no infectious force before entering the infectious class I. In this case, only infectious individuals in class I can transmit the infection. As before, let $\theta(t)$ be the probability that a randomly chosen edge has not transmitted infection by time t . Then, the fraction of nodes that are susceptible at time t is

$$S(t) = \sum_{k=0}^{\infty} P(k)\theta(t)^k = \Psi(\theta(t)). \quad (6)$$

To understand the efficiency that a randomly chosen node gets infectious, we need to introduce another two augmented variables. Denote by ϕ_I the probability that an edge has not transmitted infection and its base node is infectious at time t , and denote by ϕ_E the probability that an edge has not transmitted infection and its base node is exposed at time t . Then,

$$\theta' = -\beta\phi_I. \quad (7)$$

On one hand, an edge associated with susceptible target and base nodes begins to satisfy the definition of ϕ_I if the base node of this edge becomes infectious, which happens at a rate $v\phi_E$. On the other hand, an edge no longer satisfies the definition for ϕ_I either because an infection crosses this edge or because the infectious base node recovers. Thus, we have

$$\phi'_I = v\phi_E - (\beta + \gamma)\phi_I. \quad (8)$$

To close the above system, we need the equation for ϕ_E . Note that an edge associated with susceptible target and base nodes begins to satisfy the definition for ϕ_E only if the base node of this edge becomes exposed, which happens at a rate $-h'(t)$, where $h(t) = \Psi'(\theta)/\Psi'(1)$ is the probability that the base node is susceptible. On the contrary, an edge no longer satisfies the definition for ϕ_E only if the exposed base node becomes infectious. Then, we have

$$\phi'_E = \beta\phi_I \frac{\Psi''(\theta)}{\Psi'(1)} - v\phi_E. \quad (9)$$

Once a susceptible node stops being the susceptible, it must first enter the exposed class E . Thus,

$$E' = -S' - vE = \beta\phi_I\Psi'(\theta) - vE. \quad (10)$$

Accordingly, the equation for the fraction of infectious nodes I is given by

$$I' = vE - \gamma I. \quad (11)$$

Eqs. (6)–(11) give the full SEIR model without infectious force in latent period. This system is completed with the following initial conditions: $\theta(0) = 1$, $\phi_E(0) = E(0) = \xi_1$, and $\phi_I(0) = I(0) = \xi_2$, where $0 \leq \xi_1, \xi_2 \ll 1$, and $S(0) + E(0) + I(0) + R(0) = 1$.

To determine the basic reproduction number R_0 for the above model, we use the next generation matrix recipe [36,37]. This method only involves the infected compartments ϕ_E and ϕ_I . Let $x = (\theta, \phi_E, \phi_I)$, and note that the disease-free equilibrium is $(1, 0, 0)$. Then, the new infection matrix F and the transition matrix V are respectively defined as

$$F = \begin{pmatrix} 0 & \beta \frac{\Psi''(1)}{\Psi'(1)} \\ 0 & 0 \end{pmatrix}, \quad V = \begin{pmatrix} v & 0 \\ -v & \beta + \gamma \end{pmatrix}.$$

Following [36,37], the basic reproduction number R_0 is defined as $\rho(FV^{-1})$, where $\rho(\cdot)$ denotes the spectral radius of a matrix. Thus,

$$R_0 = \frac{\beta}{\beta + \gamma} \frac{\Psi''(1)}{\Psi'(1)}. \quad (12)$$

The above expression of R_0 is the same as (5) for SIR model on random networks, which shows that the SEIR model without infectious force in latent period doesn't alter the disease threshold $R_0 = 1$. This is slightly different from the classic SEIR model [7,38] without infectious force in latent period and vital dynamics, which is also pointed out by Lindquist et al. [13] for SIR model on random networks.

The final epidemic size can be determined as follows. By letting $\phi'_E = E' = 0$ and $\phi'_I = I' = 0$, we have $\phi_E(\infty) = E(\infty) = 0$ and $\phi_I(\infty) = I(\infty) = 0$ at the end of the epidemic. From (9), we obtain $v\phi_E = \beta\phi_I \frac{\Psi''(\theta)}{\Psi'(1)} - \phi'_E$. Plugging this relation and $\phi_I = -\theta'/\beta$ into (8), we have

$$\phi'_I = \theta' + \frac{\gamma}{\beta}\theta' - \phi'_E - \frac{\Psi''(\theta)}{\Psi'(1)}\theta'. \quad (13)$$

Integrating (13) from 0 to t yields

$$\phi_I = \xi_1 + \xi_2 + \theta - \phi_E - \frac{\gamma}{\beta}(1 - \theta) - \frac{\Psi'(\theta)}{\Psi'(1)}, \quad (14)$$

where the initial conditions $\theta(0) = 1$, $\phi_E(0) = \xi_1$ and $\phi_I(0) = \xi_2$ are employed. Thus,

$$\theta' = -\beta\phi_I = -\beta(\xi_1 + \xi_2) - \beta\theta + \beta\phi_E + \gamma(1 - \theta) + \beta \frac{\Psi'(\theta)}{\Psi'(1)}. \quad (15)$$

Letting $\theta' = 0$ gives

$$\theta_\infty = \theta(\infty) = \frac{\beta \frac{\Psi'(\theta_\infty)}{\Psi'(1)} + \beta\phi_E(\infty) + \gamma - \beta(\xi_1 + \xi_2)}{\beta + \gamma}. \quad (16)$$

Usually, the final epidemic size is determined by assuming small initial conditions. That is, $\xi_1 \approx 0$ and $\xi_2 \approx 0$. Then,

$$\theta_\infty = \frac{\beta \frac{\Psi'(\theta_\infty)}{\Psi'(1)} + \gamma}{\beta + \gamma}, \quad (17)$$

using the fact $\phi_E(\infty) = 0$ at the end of the epidemic. Therefore, $S(\infty) = \Psi(\theta_\infty)$ and $R(\infty) = 1 - S(\infty)$.

From (12) and (17), we see that the basic reproduction number R_0 and the final epidemic size $R(\infty)$ for the SEIR model without infectious force in latent period are the same as that for the SIR model on random networks, which shows that the latent period E has no effects on the disease threshold and the final epidemic size. However, as we will see in the next section, the length of latent period $1/v$ has great impact on the arrival time of the peak and the peak size. In the limit of large v , one recovers the SIR dynamics on random networks, that is, SEIR model without infectious force in latent period reduces to the SIR model on random networks.

It should be noted that in [34] Shang formulated an SEIR model without infectious force in latent period on random networks. Adapting the notations from [34] and using the unified notations defined above, we can rewrite the model in [34] as

$$\begin{cases} \theta' = -\beta\phi_I, \\ \phi'_E = \beta\phi_I \frac{\Psi''(\theta)}{\Psi'(1)} - (\beta + v)\phi_E, \\ \phi'_I = \beta\phi_I \frac{\Psi''(\theta)}{\Psi'(1)} - \beta\phi_E - \gamma\phi_I, \\ S = \Psi(\theta), \\ E' = \beta SI - vE, \\ R' = \gamma I. \end{cases} \quad (18)$$

This model is completed with the following initial conditions [34]: $\theta(0) = 1 - \zeta_1$, $\phi_E(0) = \xi_1$ and $\phi_I(0) = \xi_2$, with $0 \leq \zeta_1, \xi_1, \xi_2 \ll 1$ in the limit of large population size. They simply mentioned the final epidemic size and didn't perform any stochastic SEIR simulations on random networks to compare with the numerical solutions of the ordinary differential Eq. (18). However, as we will see in the next section, the predictions of model (18) do not capture the stochastic SEIR simulations on random networks, while the predictions of our model do.

2.3. SEIR dynamics with infectious force in the latent period

We now consider SEIR dynamics with infectious force in latent period. Once susceptible individuals get infected, they first enter an infected phase E but simultaneously have reduced infectious force before entering the infectious class I . In this case, both individuals in class E and I can spread the disease, but individuals in class E may have no symptoms or may not be diagnosed. Through mean-field approximations [10,11], susceptible nodes of degree k evolve statistically according to the following differential equation

$$S'_k = -\beta k S_k p_I - \alpha k S_k p_E. \quad (19)$$

Here, $\alpha = \epsilon\beta$ is the reduced infectious force of individuals in latent period, and $p_I = M_{SI}/M_S$ and $p_E = M_{SE}/M_S$ are respectively the fraction of S-I (M_{SI}) and S-E (M_{SE}) edges among the total number of edges emanating from the susceptible nodes (M_S). Then, kp_I and kp_E denote the expected number of edges that a susceptible node of degree k connects to nodes in status I and E, respectively [16]. Consequently, a susceptible node of degree k becomes infected, entering the exposed phase, at time t is $\beta kp_I(t) + \alpha kp_E(t)$.

Integrating Eq. (19) from 0 to t one obtains

$$\frac{S_k(t)}{S_k(0)} = \exp \left\{ - \int_0^t [\beta kp_I(\tau) + \alpha kp_E(\tau)] d\tau \right\} = \theta(t)^k, \quad (20)$$

where $\theta(t) \doteq \exp\{-\int_0^t [\beta p_I(\tau) + \alpha p_E(\tau)] d\tau\}$ denotes the probability that a randomly chosen edge does not admit infection, neither from the exposed nodes E nor from the infected nodes I , by time t . Hence, the probability that a susceptible node of degree k at time 0 still remains susceptible at some time t is $\theta(t)^k$. Then, the total fraction of nodes that are susceptible at time t is also given by Eq. (6). To explore the dynamics for $\theta(t)$, note that both the infected nodes I and the exposed nodes E have the infectious force. Then,

$$\theta' = -\beta\phi_I - \alpha\phi_E. \quad (21)$$

The dynamic equation for ϕ_I is the same as Eq. (8) since susceptible individuals first enter the exposed class once infected. Accordingly, the dynamic equation for ϕ_E (cf. (9)) becomes

$$\phi'_E = (\beta\phi_I + \alpha\phi_E) \frac{\Psi''(\theta)}{\Psi'(1)} - (\alpha + \nu)\phi_E. \quad (22)$$

The first term of Eq. (22) represents the probability that the base node of an edge connected to a susceptible target node gets infected and enters the exposed phase, either through infected nodes I or through exposed nodes E , and the second term considers the probability that an edge no longer satisfies the definition of ϕ_E , either through transmitting the infection with constant rate α or through moving to the infected class I .

Similar argument as in the previous subsection, we have

$$E' = -S' - \nu E = (\beta\phi_I + \alpha\phi_E)\Psi'(\theta) - \nu E. \quad (23)$$

Therefore, the full system governing the SEIR dynamics with infectious force in latent period on random networks is

$$\begin{cases} \theta' = -\beta\phi_I - \alpha\phi_E, \\ \phi'_E = (\beta\phi_I + \alpha\phi_E) \frac{\Psi''(\theta)}{\Psi'(1)} - (\alpha + \nu)\phi_E, \\ \phi'_I = \nu\phi_E - (\beta + \gamma)\phi_I, \\ S = \Psi(\theta), \\ E' = (\beta\phi_I + \alpha\phi_E)\Psi'(\theta) - \nu E, \\ I' = \nu E - \gamma I. \end{cases} \quad (24)$$

This system is completed with the initial conditions: $\theta(0) = 1$, $\phi_E(0) = E(0) = \xi_1$ and $\phi_I(0) = I(0) = \xi_2$, where $0 \leq \xi_1, \xi_2 \ll 1$, and $S(0) + E(0) + I(0) + R(0) = 1$.

To compute the basic reproduction number R_0 for model (24), we use the similar method introduced in previous subsection. Similarly, the infected compartments involved are ϕ_E and ϕ_I . Using the disease-free equilibrium $x = (\theta, \phi_E, \phi_I) = (1, 0, 0)$, we define the new infection matrix F and the transition matrix V as

$$F = \begin{pmatrix} \alpha \frac{\Psi''(1)}{\Psi'(1)} & \beta \frac{\Psi''(1)}{\Psi'(1)} \\ 0 & 0 \end{pmatrix}, \quad V = \begin{pmatrix} \alpha + \nu & 0 \\ -\nu & \beta + \gamma \end{pmatrix}.$$

Then, the basic reproduction number R_0 is

$$R_0 = \rho(FV^{-1}) = \frac{\alpha}{\alpha + \nu} \frac{\Psi''(1)}{\Psi'(1)} + \frac{\nu}{\alpha + \nu} \frac{\beta}{\beta + \gamma} \frac{\Psi''(1)}{\Psi'(1)}, \quad (25)$$

where the term $\frac{\alpha}{\alpha + \nu}$ denotes the probability that an exposed node transmits the infection along a random accessible edge before it moves on to the infected class I , and the term $\frac{\nu}{\alpha + \nu} \frac{\beta}{\beta + \gamma}$ is the probability that an exposed node moves on to the infected class I and then transmits the infection along a random accessible edge before it recovers. The basic reproduction number R_0 is the sum of contributions from the exposed individuals E and infected individuals I . If $\alpha = 0$, i.e. $\epsilon = 0$, one retrieves the basic reproduction number R_0 (12) for SEIR model without infectious force in latent period. It is not difficult to get

$$\frac{\alpha}{\alpha + \nu} + \frac{\nu}{\alpha + \nu} \frac{\beta}{\beta + \gamma} \geq \frac{\beta}{\beta + \gamma},$$

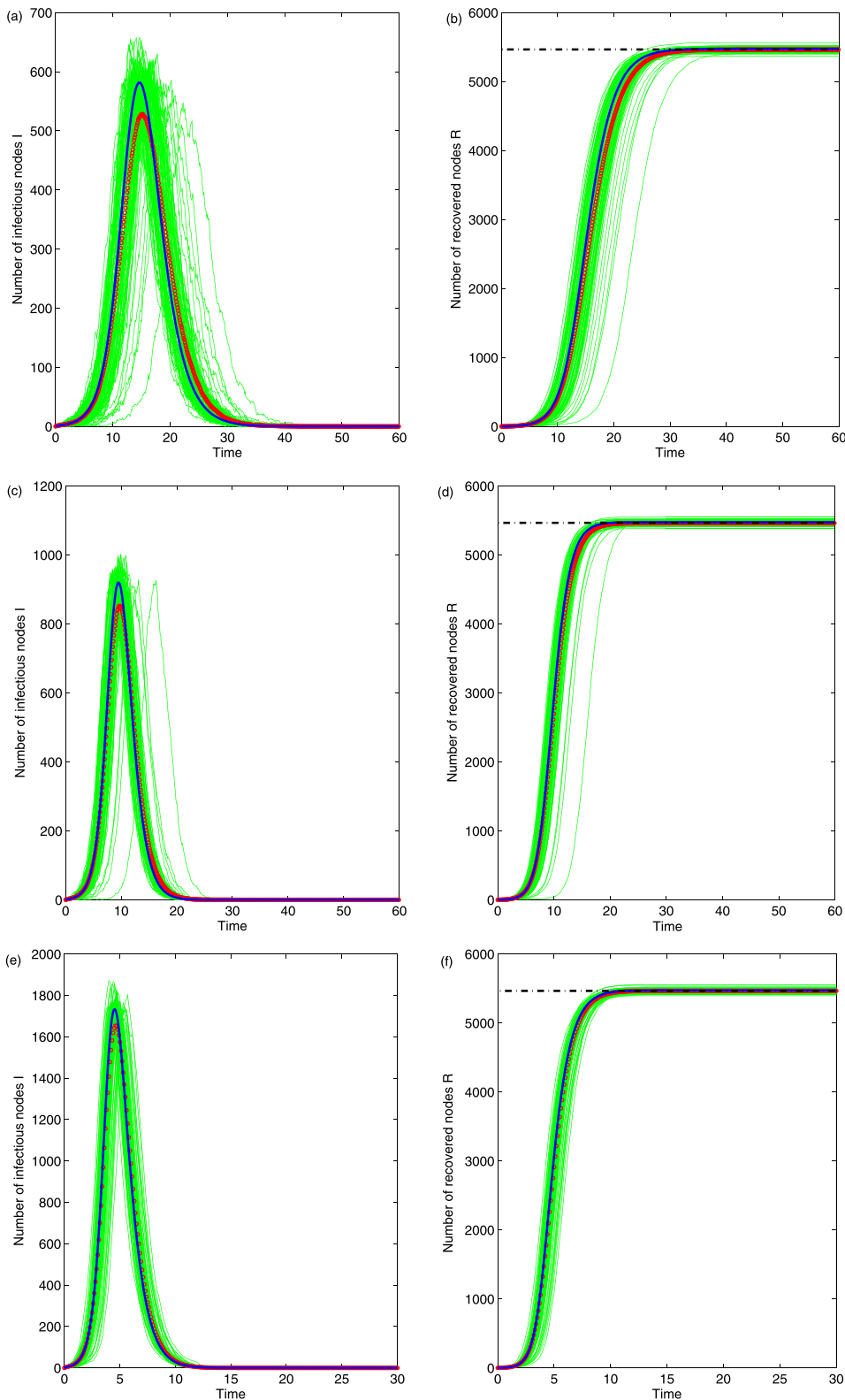


Fig. 1. The comparison of SEIR (without infectious force in latent period) ODE model predictions (blue lines) with the ensemble average (red circles) of 100 runs of stochastic simulations (green lines) on a Poisson network with $N = 6000$ and $\langle k \rangle = 6$. Disease parameters: $\beta = 0.8$, $\gamma = 1$, $\nu = 0.5$ (a, b), $\nu = 1$ (c, d), $\nu = 5$ (e, f), and initial infections $E(0) = 6$ and $I(0) = 0$. Black lines are the analytical predictions of the final size formula (17). (For interpretation of the references to colour in this figure legend, the reader is referred to the web version of this article.)

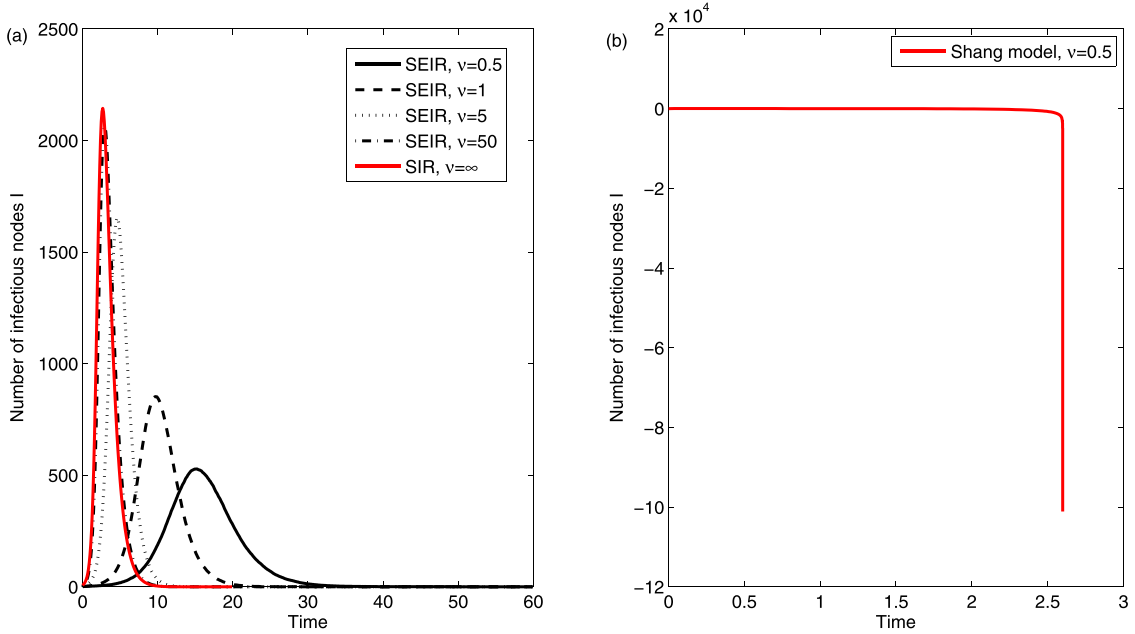


Fig. 2. (a) The comparison of SEIR (without infectious force in latent period) dynamics with the SIR dynamics by varying the latent period $1/\nu$. Each curve is the ensemble average of 100 runs of stochastic SEIR simulations. (b) The prediction of the ODE model (18) developed in [34]. Other network and disease parameters and the initial conditions are the same as that in Fig. 1.

and the equality holds if and only if $\alpha = 0$. This implies that the infectious force in latent period will increase the possibility of disease outbreak, which is consistent with our intuition and is not a good news for diseases that have infectious force in latent period without any symptom.

To determine the final epidemic size, we need some more effort. As pointed out by Ma and Earn [39], social heterogeneities, in our case the number of contacts constrained by a network, may affect the final size formula. In other words, explicit form of the final size formula for models incorporating spatial structure or social heterogeneities may deviate from the final size formula for classical SIR models [3], and they are available for some particular models. For more details about the final size formula for homogeneously mixed models or for structured models, we refer the reader to [39]. Fortunately, we can calculate the epidemic final size $R(\infty)$ for model (24).

Let $J_1 = S + E$ and $J_2 = S + E + I$, respectively. Then $J'_1 = S' + E' = -\nu E$, so $E > 0$ implies J_1 is decreasing and bounded below by zero, and $\lim_{t \rightarrow \infty} J'_1 = 0$. Hence $\phi_E(\infty) = E(\infty) = 0$. Similarly, $J'_2 = S' + E' + I' = -\gamma I$, so $I > 0$ implies J_2 is decreasing and bounded below by zero, and $\lim_{t \rightarrow \infty} J'_2 = 0$. Hence $\phi_I(\infty) = I(\infty) = 0$. Therefore, $R(\infty) = 1 - S(\infty) = 1 - \Psi(\theta_\infty)$. What we need is to determine the probability θ_∞ that a randomly chosen node u escapes from the infection at the end of the epidemic.

To this end, from the first and third equation of model (24), we have

$$\phi_E = \frac{\beta}{\beta\nu + \alpha(\beta + \gamma)} \phi'_I - \frac{\beta + \gamma}{\beta\nu + \alpha(\beta + \gamma)} \theta'. \quad (26)$$

Plugging Eq. (26) into the second equation of model (24) and using the expression $\beta\phi_I + \alpha\phi_E = -\theta'$, we have

$$\phi'_E = -\theta' \frac{\Psi''(\theta)}{\Psi'(1)} - \frac{\beta(\alpha + \nu)}{\beta\nu + \alpha(\beta + \gamma)} \phi'_I + \frac{(\beta + \gamma)(\alpha + \nu)}{\beta\nu + \alpha(\beta + \gamma)} \theta'. \quad (27)$$

Integrating the Eq. (27) from 0 to t yields

$$\phi_E = \xi_1 + 1 - \frac{\Psi'(\theta)}{\Psi'(1)} - \frac{\beta(\alpha + \nu)}{\beta\nu + \alpha(\beta + \gamma)} (\phi_I - \xi_2) - \frac{(\beta + \gamma)(\alpha + \nu)}{\beta\nu + \alpha(\beta + \gamma)} (1 - \theta), \quad (28)$$

in which the initial conditions $\theta(0) = 1$, $\phi_E(0) = \xi_1$ and $\phi_I(0) = \xi_2$ are used. Letting $t \rightarrow \infty$ and using the fact $\phi_E(\infty) = \phi_I(\infty) = 0$, we have

$$\theta_\infty = 1 - \frac{\beta\nu + \alpha(\beta + \gamma)}{(\beta + \gamma)(\alpha + \nu)} \xi_1 - \frac{\beta(\alpha + \nu)}{(\beta + \gamma)(\alpha + \nu)} \xi_2 - \frac{\beta\nu + \alpha(\beta + \gamma)}{(\beta + \gamma)(\alpha + \nu)} \left(1 - \frac{\Psi'(\theta_\infty)}{\Psi'(1)} \right). \quad (29)$$

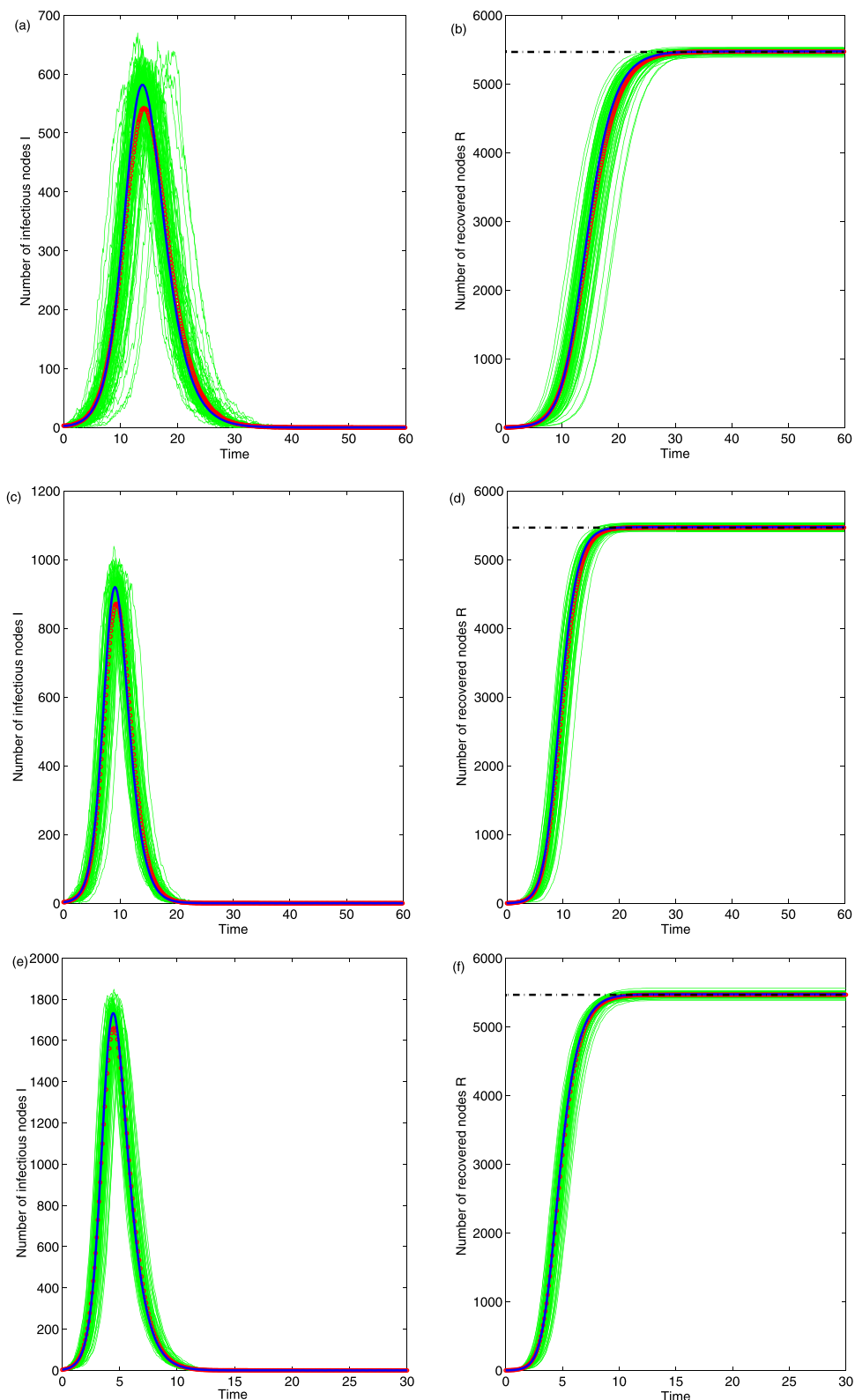


Fig. 3. The comparison of SEIR (without infectious force in latent period) ODE model predictions (blue lines) with the ensemble average (red circles) of 100 runs of stochastic simulations (green lines) on a Poisson network with $N = 6000$ and $\langle k \rangle = 6$. Disease parameters are the same as that in Fig. 1 except the initial infections $E(0) = 3$ and $I(0) = 3$. Black lines are the analytical predictions of the final size formula (17). (For interpretation of the references to colour in this figure legend, the reader is referred to the web version of this article.)

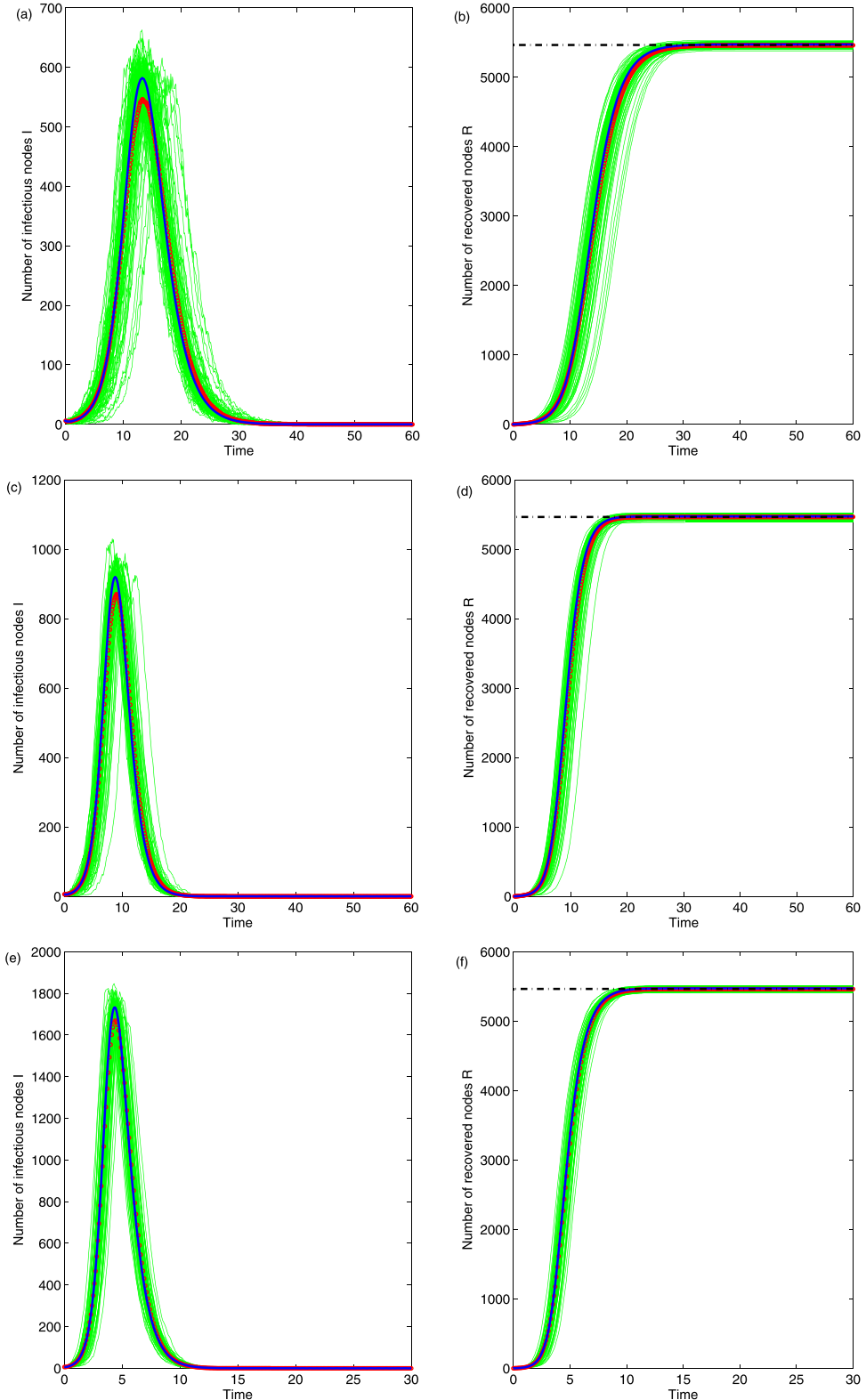


Fig. 4. The comparison of SEIR (without infectious force in latent period) ODE model predictions (blue lines) with the ensemble average (red circles) of 100 runs of stochastic simulations (green lines) on a Poisson network with $N = 6000$ and $\langle k \rangle = 6$. Disease parameters are the same as that in Fig. 1 except the initial infections $E(0) = 0$ and $I(0) = 6$. Black lines are the analytical predictions of the final size formula (17). (For interpretation of the references to colour in this figure legend, the reader is referred to the web version of this article.)

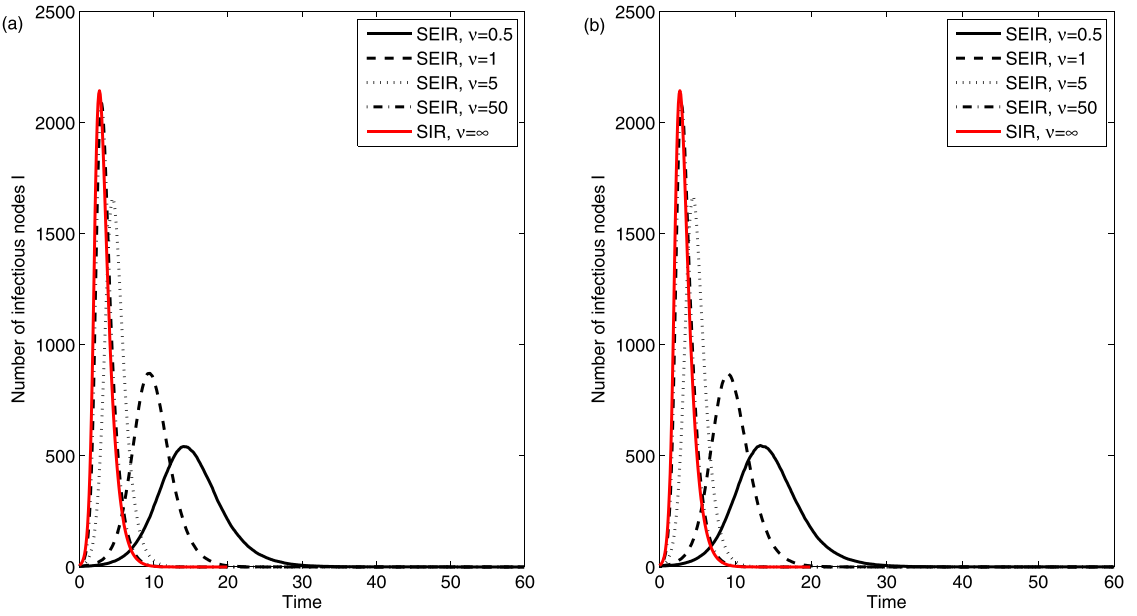


Fig. 5. The comparison of SEIR (without infectious force in latent period) dynamics with the SIR dynamics by varying the latent period $1/\nu$. Each curve is the ensemble average of 100 runs of stochastic SEIR simulations. (a) $E(0) = I(0) = 3$; (b) $E(0) = 0$ and $I(0) = 6$. Other network and disease parameters are the same as that in Fig. 1.

Hence, the final epidemic size is $R(\infty) = 1 - \Psi(\theta_\infty)$. Assuming small initial infections, i.e. $\xi_1 \approx 0$ and $\xi_2 \approx 0$, we further have

$$\theta_\infty = 1 - \frac{\beta\nu + \alpha(\beta + \gamma)}{(\beta + \gamma)(\alpha + \nu)} \left(1 - \frac{\Psi'(\theta_\infty)}{\Psi'(1)} \right).$$

Moreover, setting $\alpha = 0$, one retrieves the final epidemic size formula for the SEIR model without infectious force in latent period.

3. Simulation results

In this section, we compare large-scale stochastic simulations with the numerical predictions of SEIR ODE models with or without infectious force in latent period. In particular, we use different initial conditions of the infectives on two types of networks (Poisson and scale-free networks), and investigate the effect of varying length of latent period on epidemic spread. To this end, we first generate a random contact network using the Molloy-Reed algorithm [40]. This method does make sense since for a large population the exact contact network is unavailable, and the obtained networks are random samples of a network family which admit the same statistics such as the degree distribution (i.e., the number of contacts made by an individual). Given the information about degree distribution, we can construct a network that follows this distribution as follows: associate each node i with the number of k_i “stubs” (or “half-edges”) drawn randomly from the degree distribution $P(k)$, and then connect two uniformly chosen stubs repeatedly until no more stubs can be selected and discard the remaining stubs. During this procedure, multiple edges between the same nodes as well as self-loops connecting a node to itself can be formed, however, the probability that the multiple edges and self-loops formed is infinitesimal in the limit of large network size N [40,41]. Hence, we can ignore the multiple edges and self-loops in this process.

To simulate SEIR dynamics on a contact network, we use the continuous-time Gillespie method [42,43]. To be specific, each node is labeled by its infection status: susceptible S, exposed E, infectious I or recovered R. For SEIR dynamics without infectious force in latent period, once a susceptible individual becomes infected, it first enters the exposed class E, and it is assigned an exponentially distributed latent period with the mean $1/\nu$, during which it is infected but not yet infectious. After the latent period of this individual, it enters the infectious class I, which is capable of transmitting the infection to susceptible individuals, and it is assigned an exponentially distributed infectious period with the mean $1/\gamma$, during which contact events are generated for each of its edges with exponentially distributed waiting times of the mean $1/\beta$. At the time of contact, if the node at the other end of an edge is susceptible, then the node is labeled with exposed E; otherwise, this contact event is discarded. After the infectious period of an individual, it enters the recovered class R and plays no role in spreading the infection. The whole epidemic process is halted if there are no exposed and infectious individuals remaining in the network. For SEIR dynamics with infectious force in latent period, the only difference is that individuals in exposed class E also have the ability of transmitting the infection with a reduced factor. We modify slightly the simulation processes

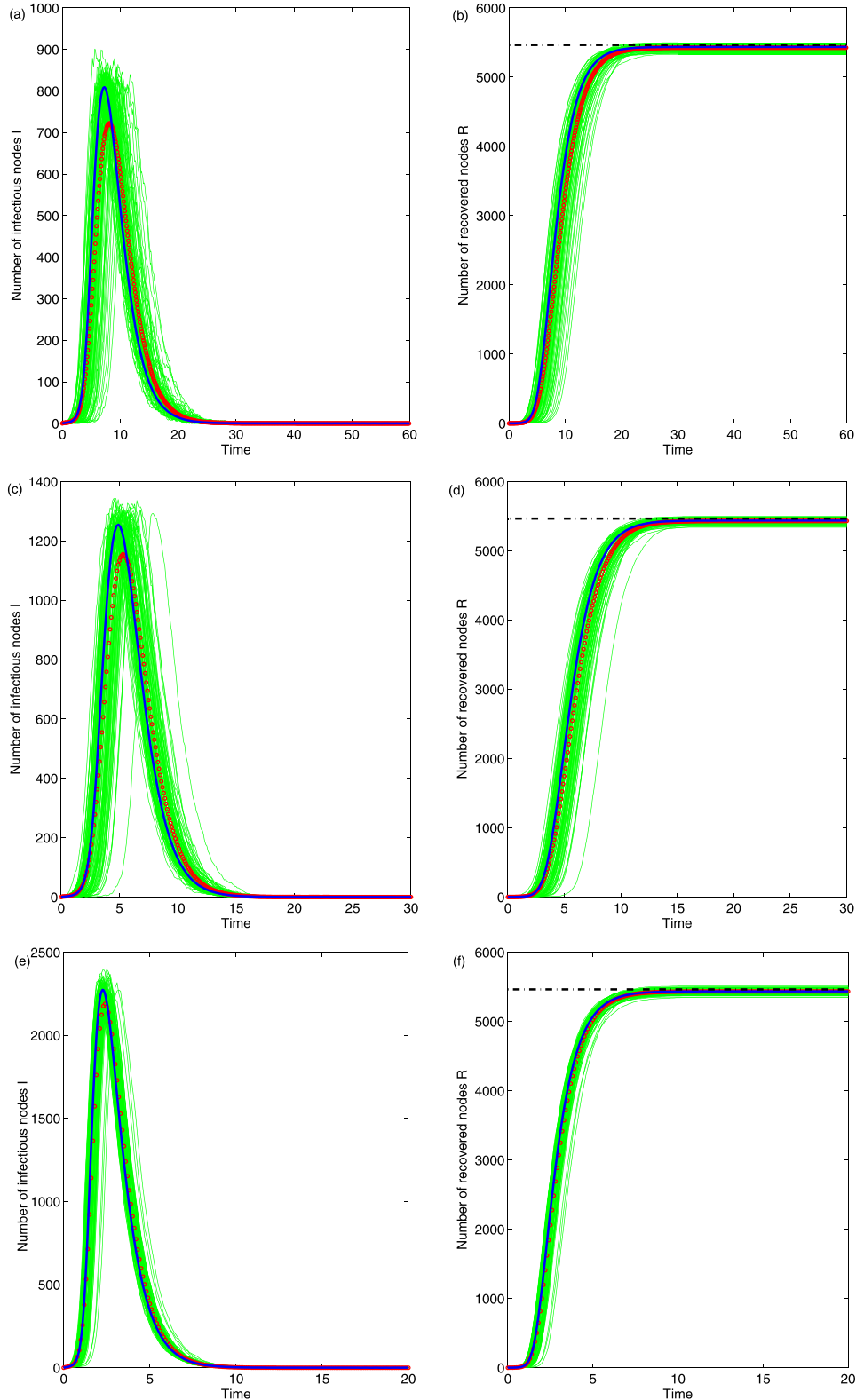


Fig. 6. The comparison of SEIR (without infectious force in latent period) ODE model predictions (blue lines) with the ensemble average (red circles) of 100 runs of stochastic simulations (green lines) on a scale-free network with $N = 6000$ and $P(k) \propto k^{-2.1}$ ($3 \leq k \leq 80$). Disease parameters: $\beta = 0.8$, $\gamma = 1$, $\nu = 0.5$ (a, b), $\nu = 1$ (c, d), $\nu = 5$ (e, f), and initial infections $E(0) = 6$ and $I(0) = 0$. Black lines are the analytical predictions of the final size formula (17). (For interpretation of the references to colour in this figure legend, the reader is referred to the web version of this article.)

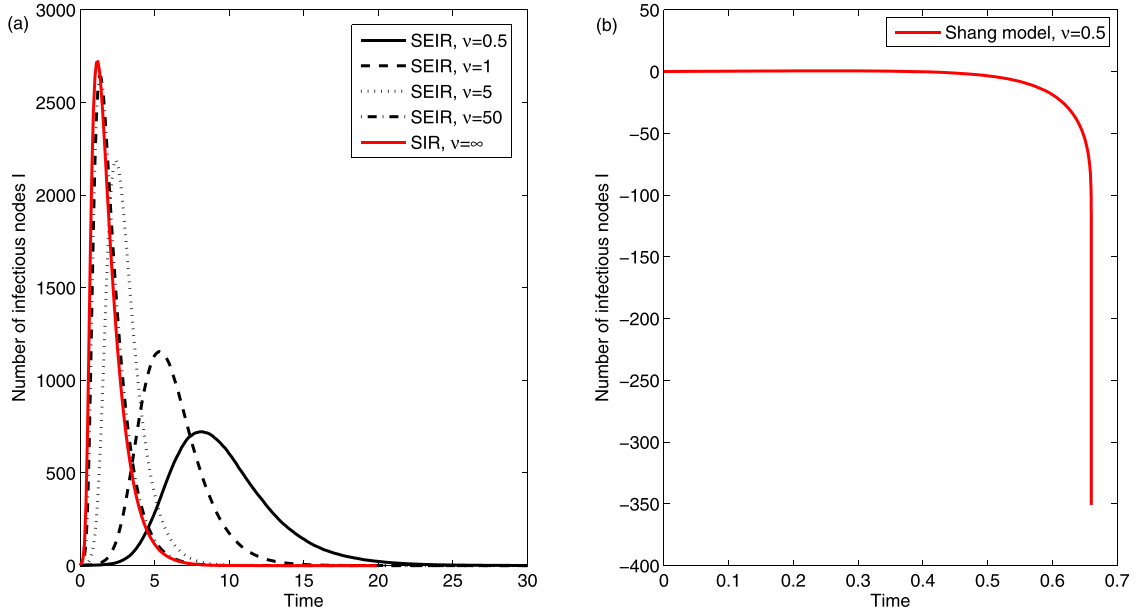


Fig. 7. (a) The comparison of SEIR (without infectious force in latent period) dynamics with the SIR dynamics by varying the latent period $1/\nu$. Each curve is the ensemble average of 100 runs of stochastic SEIR simulations. (b) The prediction of the ODE model (18) developed in [34]. Other network and disease parameters and the initial conditions are the same as that in Fig. 6.

of SEIR dynamics without infectious force in latent period as follows. During the latent period $1/\nu$, contact events are also generated for each of its edges with exponentially distributed waiting times of the mean $1/\alpha$; at the time of contact, if the node at the other end of an edge is susceptible, then the node is labeled with exposed E; otherwise, this contact event is discarded. After the latent period of an individual, it enters the infectious class I, which transmits the infection with a higher rate β ($> \alpha$).

In the following, we generate two types of contact networks: one follows the Poisson degree distribution (Poisson contact network) and the other follows the power-law degree distribution (scale-free contact network). On each network, we perform 100 independent runs of stochastic SEIR dynamics, and compare the ensemble average of simulation results with the corresponding numerical solutions of SEIR ODE models using the same contact network and disease parameters. What we are interested is the deterministic epidemic (i.e., an epidemic is established in the population), so we adopt a relatively large initial infections.

In all the simulations, we fix the disease parameters $\beta = 0.8$ and $\gamma = 1$, and vary the latent periods $1/\nu$ and initial conditions to see how they affect the epidemic evolution on different networks. In Fig. 1, we show the SEIR dynamics without infectious force in latent period on a Poisson network with all the initial infections being exposed under different latent period $1/\nu$. Simulation results reveal that our model predictions about the epidemic evolution and the final epidemic size agree well with the ensemble averages of the stochastic simulations. To obtain the analytical predictions of the final size, we recall the formula (17). Note that $\theta_\infty = 1$ is an equilibrium corresponding to the disease-free state. What we want is an equilibrium $0 < \theta_\infty < 1$ at the end of the epidemic, so we compute θ_∞ iteratively. Specifically, we use the following iterative formula

$$\theta_{n+1} = \frac{\beta \frac{\Psi'(\theta_n)}{\Psi'(1)} + \gamma}{\beta + \gamma}, \quad n = 1, 2, 3, \dots. \quad (30)$$

We can chose arbitrary value $\theta_1 \in (0, 1)$ as an initial value. For example, we set $\theta_1 = 0.8$, and obtain $\theta_\infty = 0.59466150$ after 25 iterative steps without any change. Then, the final epidemic size is $N(1 - \Psi(\theta_\infty)) \approx 5465$. Fig. 1(b), (d) and (f) show that the analytical predictions (black lines) of the final epidemic size agree very well with the ODE model predictions and stochastic simulations. As the latent period increases, the epidemic peak becomes lower, the arrival of the peak delays, and the fluctuations becomes stronger (cf. Fig. 1(a) $1/\nu = 2$, (c) $1/\nu = 1$ and (e) $1/\nu = 0.2$). In the limit of large ν , the SEIR dynamics without infectious force in latent period converges to the SIR dynamics. To see this, we show stochastic SEIR simulation results in Fig. 2(a) with different lengths of latent period. From Fig. 2(a), we can see that as the length of latent period decreases, the SEIR dynamics is more close to SIR dynamics; when $\nu = 50$, the curve of SEIR dynamics is indistinguishable from that of SIR dynamics. Fig. 2(b) shows the prediction of ODE model (18) developed in [34]. As can be seen, model (18) provides neither a quantitative nor a qualitative prediction of the epidemic evolution. In fact, numerical solution of the ODE model (18) diverges quickly, and becomes negative, which shows that model (18) is not well-posed. Thus, we will not show the comparison of model (18) prediction with the stochastic SEIR simulations on the Poisson network.

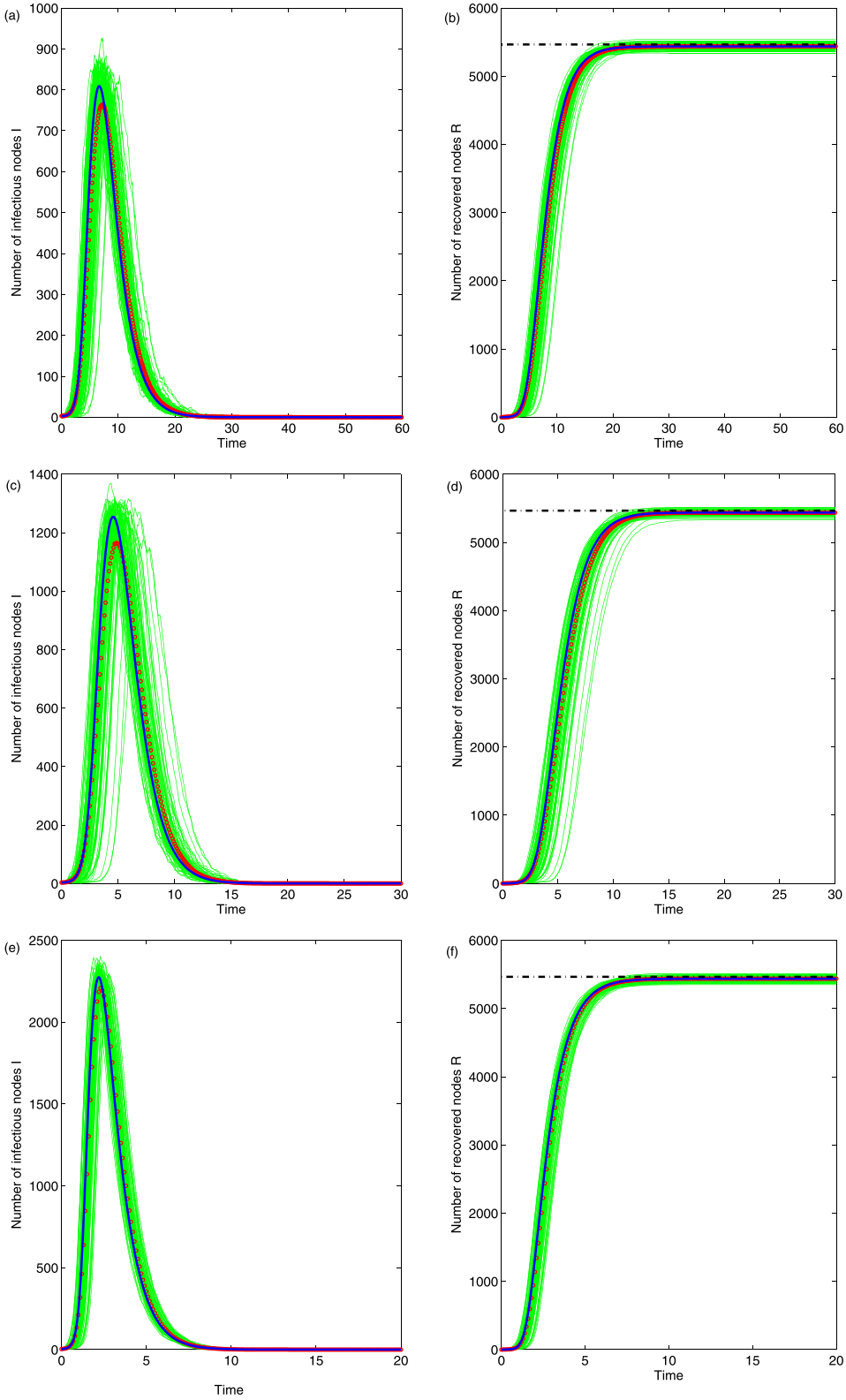


Fig. 8. The comparison of SEIR (without infectious force in latent period) ODE model predictions (blue lines) with the ensemble average (red circles) of 100 runs of stochastic simulations (green lines) on a scale-free network with $N = 6000$ and $P(k) \propto k^{-2.1}$ ($3 \leq k \leq 80$). Disease parameters are the same as that in Fig. 6 except the initial infections $E(0) = 3$ and $I(0) = 3$. Black lines are the analytical predictions of the final size formula (17). (For interpretation of the references to colour in this figure legend, the reader is referred to the web version of this article.)

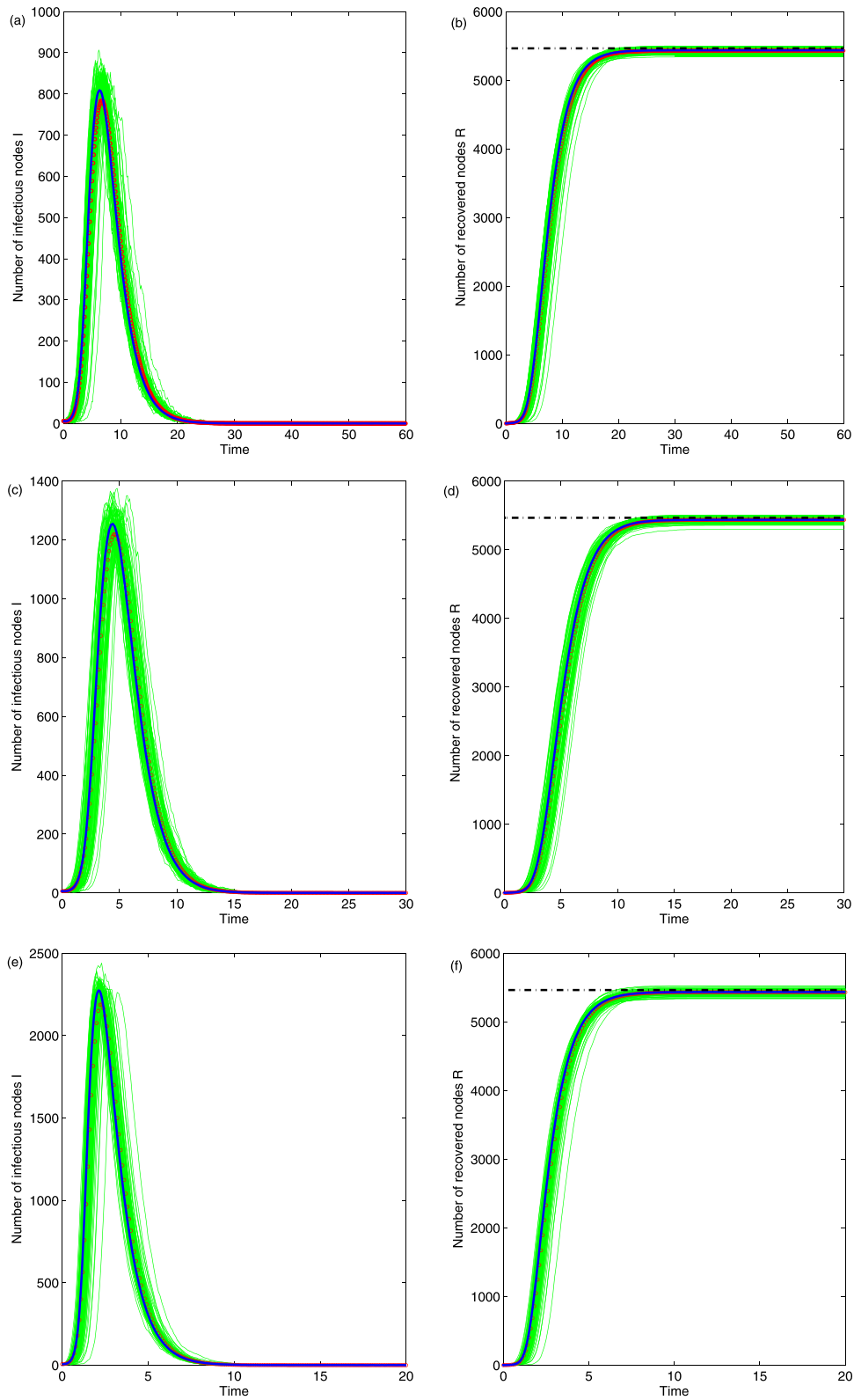


Fig. 9. The comparison of SEIR (without infectious force in latent period) ODE model predictions (blue lines) with the ensemble average (red circles) of 100 runs of stochastic simulations (green lines) on a scale-free network with $N = 6000$ and $P(k) \propto k^{-2.1}$ ($3 \leq k \leq 80$). Disease parameters are same as that in Fig. 6 except the initial infections $E(0) = 0$ and $I(0) = 6$. Black lines are the analytical predictions of the final size formula (17). (For interpretation of the references to colour in this figure legend, the reader is referred to the web version of this article.)

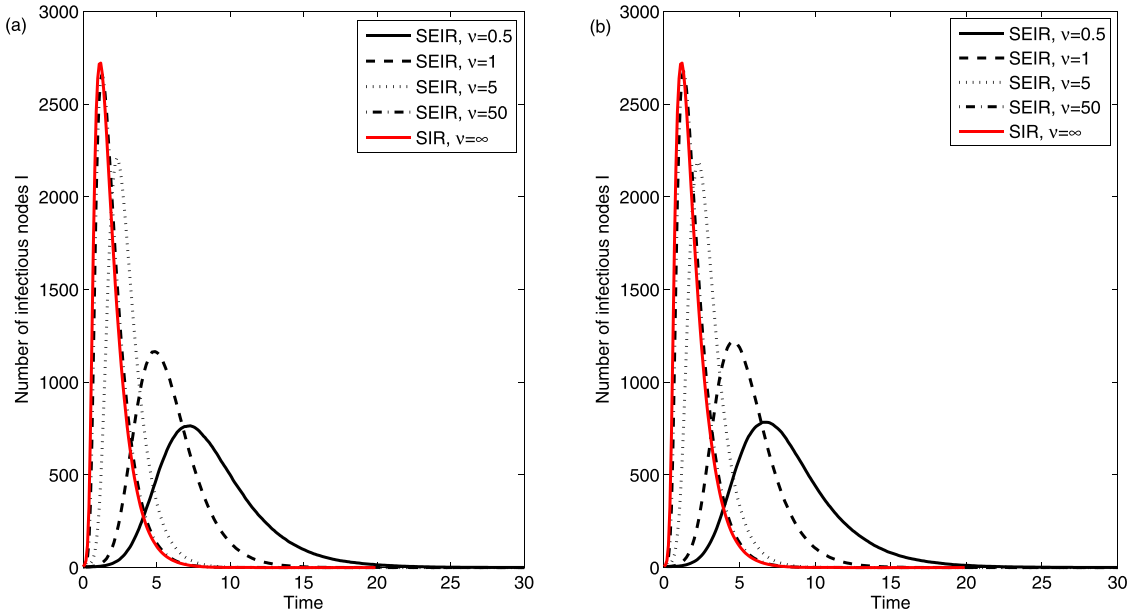


Fig. 10. The comparison of SEIR (without infectious force in latent period) dynamics with the SIR dynamics by varying the latent period $1/v$. Each curve is the ensemble average of 100 runs of stochastic SEIR simulations. (a) $E(0) = I(0) = 3$; (b) $E(0) = 0$ and $I(0) = 6$. Other network and disease parameters and the initial conditions are the same as that in Fig. 6.

In Figs. 3 and 4, we compare the ODE model predictions with the stochastic SEIR simulations by using the same network and disease parameters as that in Fig. 1 but different initial conditions, and we observe similar behavior as those in Fig. 1. However, we note that if the length of latent period becomes longer (cf. Figs. 1(a), 3(a) and 4(a)), then there would be much more stochastic fluctuations in the simulation curves, and these fluctuations become stronger with the length of latent period increasing. Hence, if we want to use stochastic simulations to predict the evolution of disease with latent period, we need perform a large number of simulations to eliminate the stochastic fluctuations. This requires considerable computational resources especially for a large population size. On the contrary, our analytical model gives more direct observations without loosing too much details.

Moreover, from Figs. 1, 3 and 4 (the second column), we can see that the final epidemic size is indeed independent of the length of latent period and the initial infections that we place randomly on the network. Our analytical prediction (17) of the final epidemic size agrees very well with the stochastic simulations. In Fig. 5, we show that, independent of initial infections, in the limit of large v the SEIR dynamics converges to the SIR dynamics.

On the other hand, many empirical data reveal that most of the real-world networks follow the power-law distributions [44], i.e. $P(k) \propto k^{-l}$, where l is the power-law exponent. Thus, in Figs. 6, 8 and 9 we also compare the ODE model predictions with the stochastic SEIR simulations on a scale-free network by varying the length of latent period and initial infections. Simulation results show that our model predictions agree well with the stochastic simulations, and the epidemic peak becomes lower, the arrival of the peak delays, and the fluctuations becomes stronger (cf. Fig. 6(a) $1/v = 2$, (c) $1/v = 1$ and (e) $1/v = 0.2$) with increasing the length of latent period $1/v$. Different from the Poisson network, the scale-free network is more robust to stochastic fluctuations in longer latent period (cf. Fig. 1(a) and 6(a)), and is more benefit for epidemic spreading since the arrival time of the peak is earlier (to emphasize this, we amplify the time axis for scale-free network) and the peak size is larger. To get the final epidemic size in scale-free network, we set $\theta_1 = 0.8$, and obtain $\theta_\infty = 0.58696004$ after 20 iterative steps without any change. Then the final epidemic size in scale-free network is $N(1 - \Psi(\theta_\infty)) \approx 5428$.

In Figs. 7(a) and 10, we show that, independent of the initial infections, the SEIR dynamics without infectious force in latent period on scale-free network converges to the corresponding SIR dynamics in the limit of large v . Fig. 7(b) shows that the model developed in [34] is also not well-posed for scale-free network.

For the SEIR model with infectious force in latent period, we let the reduced factor $\epsilon = 0.625$, i.e. $\alpha = 0.5$. From Figs. 11 and 12, we can see that the predictions of our SEIR model (24) agree very well with the ensemble average of 100 runs of stochastic simulations on both Poisson and scale-free networks. Since the simulation results with different initial infections are similar, so we only present the results with $E(0) = I(0) = 3$. To calculate the final epidemic size, recalling the formula (29) we need the following iterative formula

$$\theta_{n+1} = 1 - \frac{\beta\nu + \alpha(\beta + \gamma)}{(\beta + \gamma)(\alpha + \nu)} \left(1 - \frac{\Psi'(\theta_n)}{\Psi'(1)}\right), \quad n = 1, 2, 3, \dots . \quad (31)$$

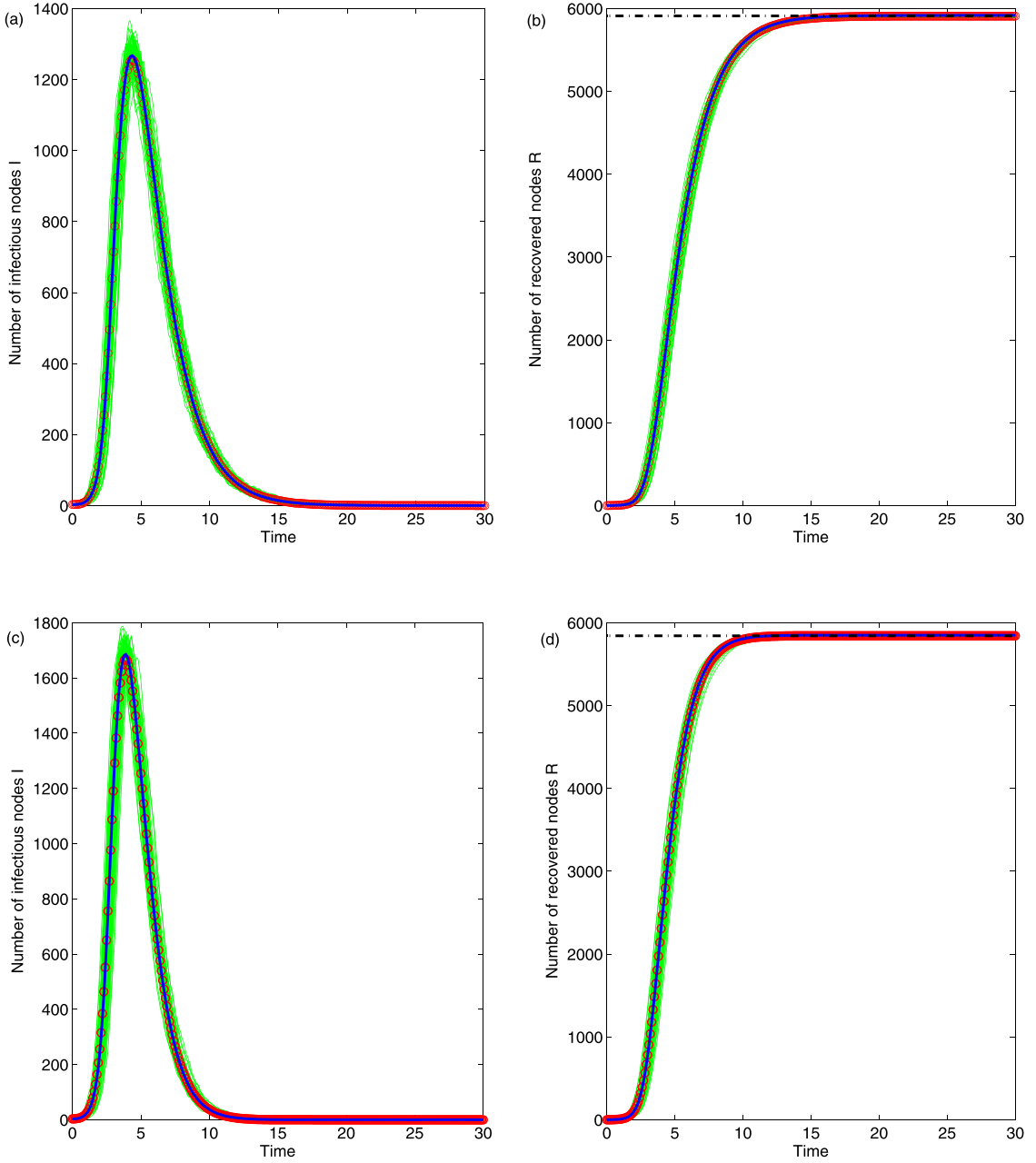


Fig. 11. The comparison of SEIR (with infectious force in latent period) ODE model (24) predictions (blue lines) with the ensemble average (red circles) of 100 runs of stochastic simulations (green lines) on a Poisson network with $N = 6000$ and $\langle k \rangle = 6$. Disease parameters: $\alpha = 0.5$, $\beta = 0.8$, $\gamma = 1$, $v = 0.5$ (a, b), $v = 1$ (c, d), and initial infections $E(0) = I(0) = 3$. Black lines are the analytical predictions of the final size formula (29). (For interpretation of the references to colour in this figure legend, the reader is referred to the web version of this article.)

For example, letting $\theta_1 = 0.8$, then for the Poisson network $\theta_\infty = 0.28805341$ after about 10 iterative steps without any change and $R(\infty) \approx 5910$ when $v = 0.5$ and $\theta_\infty = 0.38639845$ after about 20 iterative steps without any change and $R(\infty) \approx 5842$ when $v = 1$; while for the scale-free network $\theta_\infty = 0.28620092$ after about 15 iterative steps without any change and $R(\infty) \approx 5948$ when $v = 0.5$ and $\theta_\infty = 0.38511690$ after about 20 iterative steps without any change and $R(\infty) \approx 5865$ when $v = 1$. For both these networks, our analytical predictions of the final epidemic size agree very well with the simulation results (cf. Figs. 11 and 12(b,d)). Also, the length of latent period has impact on the final epidemic size. Specifically, as the length of latent period increases, more people would be affected by the epidemic because the exposed individuals can also transmit the disease.

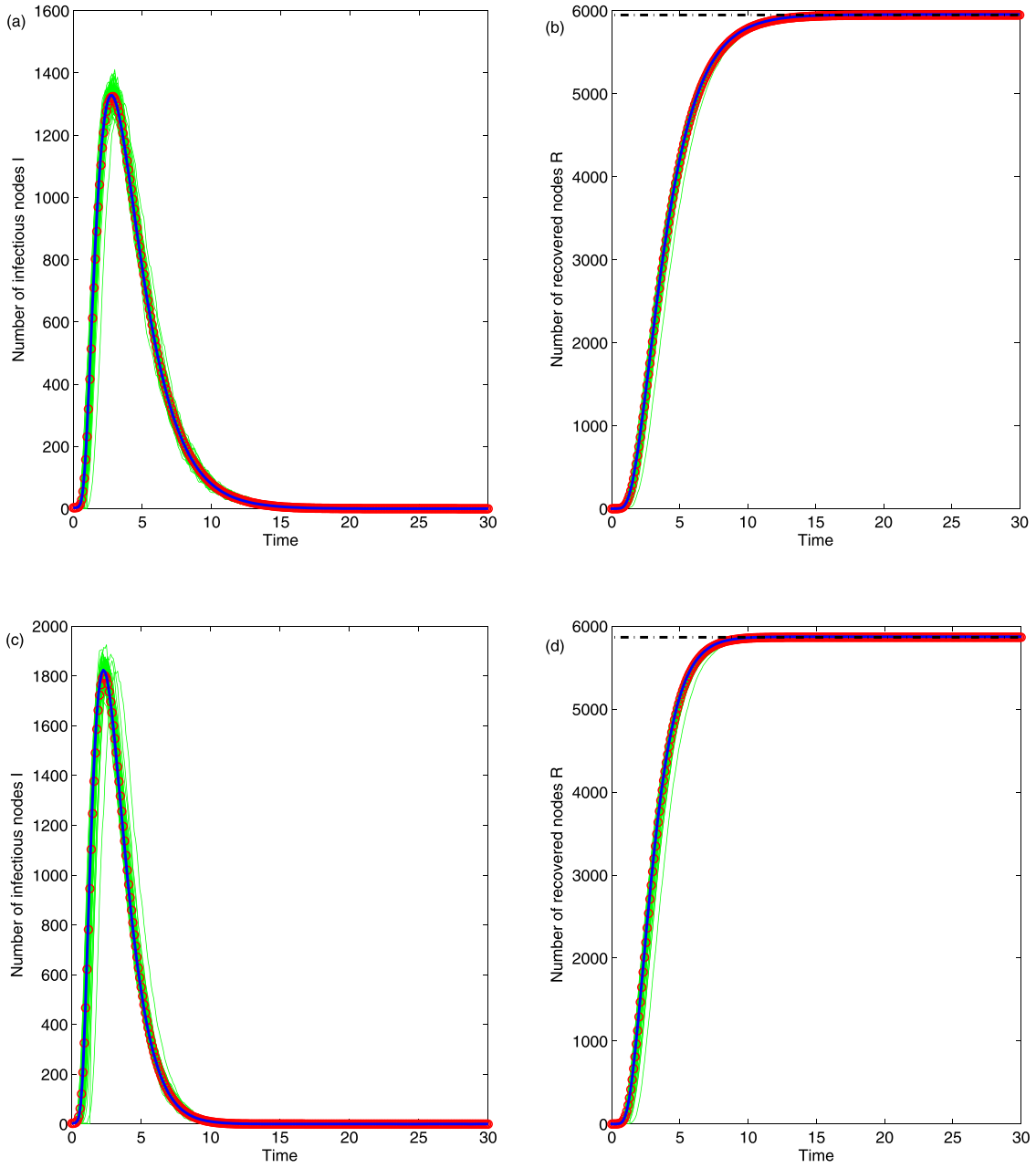


Fig. 12. The comparison of SEIR (with infectious force in latent period) ODE model (24) predictions (blue lines) with the ensemble average (red circles) of 100 runs of stochastic simulations (green lines) on a scale-free network with $N = 6000$ and $P(k) \propto k^{-2.1}$ ($3 \leq k \leq 80$). Disease parameters: $\alpha = 0.5$, $\beta = 0.8$, $\gamma = 1$, $\nu = 0.5$ (a, b), $\nu = 1$ (c, d), and initial infections $E(0) = I(0) = 3$. Black lines are the analytical predictions of the final size formula (29). (For interpretation of the references to colour in this figure legend, the reader is referred to the web version of this article.)

4. Concluding remarks

It has been observed that many diseases have latent periods, that is, individuals first enter an exposed phase E without any apparent symptoms, before entering an infectious class I . In the existing literatures, the homogeneously mixed SEIR models with or without vital dynamics ((births and deaths) have been widely investigated [24–28]. However, the SEIR dynamics on networks is not well understood. At the first glance, most of the networks look as if they were spun randomly. In other words, only the information about degree distribution, i.e. the number of contacts made by an individual, is available. Thus, we can draw a random network from the samples of a network family that follows the same degree distribution, and study the epidemic dynamics on random networks.

In summary, we have considered and analyzed the SEIR dynamics with or without infectious force in latent period on random networks in detail. By using the probability generating functions, both of these models are governed with nonlinear systems of intrinsically three dimensional ordinary differential equations, which have the same dimension as the classical SEIR models. The explicit basic reproduction numbers and the final epidemic size formulae are derived. For the SEIR model without infectious force in latent period, although the length of latent period has no influence on the basic reproduction number and the final epidemic size, it has great impact on the arrival time of the peak and the peak size. For the SEIR model with infectious force in latent period, the length of latent period also affects the basic reproduction number and the final epidemic size. Moreover, we conduct large-scale stochastic SEIR simulations using the continuous-time Gillespie method. Simulation results show that, independent of the initial infections, the model predictions agree well with the ensemble average of 100 runs of stochastic simulations, and the analytical final size formulae are verified. For the SEIR model without infectious force in latent period on random networks, the SEIR dynamics reduces to the SIR dynamics in the limit of large v , which is also verified by our simulations. It should be noted that network topology also has great effect on the epidemic dynamics including the arrival time of the peak, the peak size and the final epidemic size, which can be seen from the time evolution of epidemic on Poisson and scale-free networks (see figures in the previous section).

For the SEIR model with infectious force in latent period on random networks, the data on the number of contacts made by individuals are easy to gather and in most cases only the data on infectious individuals with obvious symptoms in class I are available, which can be used to estimate the disease parameters [31]. On one hand, our model can be extended to model infectious diseases having multi-stage infections [19] or having a carrier class such as hepatitis [45]. For all these extensions, random network models are good starting points. On the other hand, only the SEIR dynamics on random networks was well captured and understood can we add more structures such as degree correlations [46] and clustering or household structure [47], to see how much these alter the epidemic behavior on the non-random networks. Other than the network properties themselves like degree correlation and cluster, human behavior also play an important role in epidemic spread on contact networks [48,49], such as vaccination and reshuffling contacts (adaptive networks); hence, the combination of game theoretical modeling [50] and contact networks would be more appropriate for a realistic epidemic spreading in human population. These and some other related issues are left for future research.

Acknowledgments

This work was partially supported by the National Natural Science Foundation of China under Grant Nos. 61272530 and 11072059, the Specialized Research Fund for the Doctoral Program of Higher Education under Grant 20110092110017, and the Natural Science Foundation of Jiangsu Province of China under Grant BK2012741. Y. Wang also acknowledges support from the Scientific Research Foundation of Graduate School of Southeast University YBJJ1330, the JSPS Innovation Program under Grant KYZZ_0062, and China Scholarship Council (CSC2014).

References

- [1] Bernoulli D. Essai d'une nouvelle analyse de la mortalité causée par la petite vérole. *Mém Math Phys Acad Roy Sci Paris* 1760;62:39–64.
- [2] Ross R. The prevention of malaria. London: John Murray; 1911.
- [3] Kermack WO, McKendrick AG. A contribution to the mathematical theory of epidemics. *Proc Royal Soc London B* 1927;115:700–21.
- [4] Diekmann O, Heesterbeek JAP, Metz JA. On the definition and the computation of the basic reproduction ratio r_0 in models for infectious diseases in heterogeneous populations. *J Math Biol* 1990;28:365–82.
- [5] Dietz K. The estimation of the basic reproduction number for infectious diseases. *Stat Methods Med Res* 1993;2:23–41.
- [6] Heesterbeek JAP, Dietz K. The concept of r_0 in epidemic theory. *Statist Neerlandica* 1996;50:89–110.
- [7] Anderson RM, May RM. Infectious diseases of humans. Oxford: Oxford University Press; 1992.
- [8] Keeling MJ, Rohani P. Modeling infectious diseases in humans and animals. Princeton: Princeton University Press; 2008.
- [9] Diekmann O, De Jong MCM, Metz JA. A deterministic epidemic model taking account of repeated contacts between the same individuals. *J Appl Prob* 1998;35:448–62.
- [10] Pastor-Satorras R, Vespignani A. Epidemic spreading in scale-free networks. *Phys Rev Lett* 2001;86:3200–3.
- [11] Moreno Y, Pastor-Satorras R, Vespignani A. Epidemic outbreaks in complex heterogeneous networks. *Eur Phys J B* 2002;26:521–9.
- [12] Newman MEJ. Spread of epidemic disease on networks. *Phys Rev E* 2002;66:016128.
- [13] Lindquist J, Ma JL, van den Driessche P, Willeboordse FH. Effective degree network disease models. *J Math Biol* 2011;62:143–64.
- [14] Keeling MJ. The effects of local spatial structure on epidemiological invasions. *Proc Roy Soc B* 1999;266:859–67.
- [15] Eames KTD, Keeling MJ. Modeling dynamic and network heterogeneities in the spread of sexually transmitted diseases. *Proc Natl Acad Sci USA* 2002;99:13330–5.
- [16] Volz E. SIR dynamics in random networks with heterogeneous connectivity. *J Math Biol* 2008;56:293–310.
- [17] Mille JC. A note on a paper by erik volz: SIR dynamics in random networks. *J Math Biol* 2011;62:349–58.
- [18] Miller JC, Slim AC, Volz EM. Edge-based compartmental modelling for infectious disease spread. *J R Soc Interface* 2012;9:890–906.
- [19] Miller JC, Volz EM. Incorporating disease and population structure into models of SIR disease in contact networks. *PLoS One* 2013;8:e69162.
- [20] Miller JC. Epidemics on networks with large initial conditions or changing structure. *PLoS One* 2014;9:e101421.
- [21] Koch D, Illner R, Ma JL. Edge removal in random contact networks and the basic reproduction number. *J Math Biol* 2013;67:217–38.
- [22] Li ML, Ma JL, van den Driessche P. Model for disease dynamics of a waterborne pathogen on a random network. *J Math Biol* 2014. doi:10.1007/s00285-014-0839-y.
- [23] Murray JD. Mathematical biology I: an introduction, vol. 17. New York: Springer; 2002. p. 315–27.
- [24] Li MY, Muldowney JS. Global stability for the SEIR model in epidemiology. *Math Biosci* 1995;125:155–64.
- [25] Li MY, Smith HL, Wang L. Global dynamics of an SEIR epidemic model with vertical transmission. *SIAM J Appl Math* 2001;62:58–69.
- [26] Zhang J, Ma ZE. Global dynamic of SEIR epidemic model with saturating contact rate. *Math Biosci* 2003;185:15–32.
- [27] Li GH, Wang WD, Jin Z. Global stability of an SEIR epidemic model with constant immigration. 30. *Chaos, Solitons & Fractals*; 2006. p. 1012–19.
- [28] Xu R, Ma ZE. Global stability of a delayed SEIRS epidemic model with saturation incidence rate. *Nonlinear Dyn* 2010;61:229–39.
- [29] Brauer F. The kermack-mckendrick epidemic model revisited. *Math Biosci* 2005;198:119–31.

- [30] Liu JL, Zhang TL. Epidemic spreading of an SEIRS model in scale-free networks. *Commun Nonlinear Sci Numer Simulat* 2011;16:3375–84.
- [31] Jin Z, Zhang JP, Song LP, Sun G-Q, Kan JL, Zhu HP. Modelling and analysis of influenza a (h1n1) on networks. *BMC Public Health* 2011;11:S9.
- [32] Stehlé J, Voirin N, Barrat A, Cattuto C, Colizza V. Simulation of an SEIR infectious disease model on the dynamic contact network of conference attendees. *BMC Medicine* 2011;9:87.
- [33] Zhu GH, Fu XC, Chen GR. Spreading dynamics and global stability of a generalized epidemic model on complex heterogeneous networks. *Appl Math Model* 2012;36:5808–17.
- [34] Shang YL. SEIR epidemic dynamics in random networks. *ISRN Epidemiol* 2013;2013:1–5. ID: 345618
- [35] Wang Y, Cao JD, Alofi A, Al-Mazrooei A, Elaiw A. Revisiting node-based SIR models in complex networks with degree correlations. *Physica A* 2015;437:75–88.
- [36] van den Driessche P, Watmough J. Reproduction numbers and sub-threshold endemic equilibria for compartmental models of disease transmission. *Math Biosci* 2002;180:29–48.
- [37] Diekmann O, Heesterbeek JAP, Roberts MG. The construction of next-generation matrices for compartmental epidemic models. *J R Soc Interface* 2010;7:873–85.
- [38] Takeuchi Y, Iwasa Y, Sato K. Mathematics for life science and medicine. Berlin: Springer; 2007.
- [39] Ma JL, Earn DJD. Generality of the final size formula for an epidemic of a newly invading infectious disease. *Bull Math Biol* 2006;68:679–702.
- [40] Molloy M, Reed B. A critical point for random graphs with a given degree sequence. *Random Struct Algor* 1995;6:161–80.
- [41] Newman MEJ, Strogatz SH, Watts DJ. Random graphs with arbitrary degree distributions and their applications. *Phys Rev E* 2001;64:026118.
- [42] Gillespie DT. A general method for numerically simulating the stochastic time evolution of coupled chemical reactions. *J Comput Phys* 1976;22:403–34.
- [43] Gillespie DT. Exact stochastic simulation of coupled chemical reactions. *J Phys Chem* 1977;81:2340–61.
- [44] Clauset A, Shalizi CR, Newman MEJ. Power-law distributions in empirical data. *SIAM Rev* 2009;51:661–703.
- [45] Cao JD, Wang Y, Alofi A, Al-Mazrooei A, Elaiw A. Global stability of an epidemic model with carrier state in heterogeneous networks. *IMA J Appl Math* 2015;80:1025–48.
- [46] Boguna M, Pastor-Satorras R. Epidemic spreading in correlated complex networks. *Phys Rev E* 2002;66:047104.
- [47] Volz EM, Miller JC, Galvani A, Meyers LA. Effects of heterogeneous and clustered contact patterns on infectious disease dynamics. *PLoS Comput Biol* 2011;7:e1002042.
- [48] Zhang HF, Xie JR, Tang M, Lai YC. Suppression of epidemic spreading in complex networks by local information based behavioral responses, 24. *Chaos*; 2014. p. 043106.
- [49] Zhang HF, Wu ZX, Tang M, Lai YC. Effects of behavioral response and vaccination policy on epidemic spreading – an approach based on evolutionary-game dynamics. *Sci Rep* 2014;4:05666.
- [50] Zhang HF, Yang ZM, Wu ZX, Wang BH, Zhou T. Braess's paradox in epidemic game: Better condition results in less payoff. *Sci Rep* 2013;3:03292.